

# Spin nematic state as a candidate of the hidden order phase of URu<sub>2</sub>Si<sub>2</sub>

Satoshi Fujimoto<sup>1</sup>

<sup>1</sup>*Department of Physics, Kyoto University, Kyoto 606-8502, Japan*

(Dated: October 29, 2018)

Motivated by the recent discovery of broken four-fold symmetry in the hidden order phase of URu<sub>2</sub>Si<sub>2</sub>[R. Okazaki et al., *Science* **331**, 439 (2011)], we examine a scenario of a spin nematic state as a possible candidate of the hidden order phase. We demonstrate that the scenario naturally explains most of experimental observations, and furthermore, reproduces successfully the temperature dependence of the spin anisotropy detected by the above-mentioned experiment in a semi-quantitative way. This result provides strong evidence for the realization of the spin nematic order.

PACS numbers:

The heavy fermion compound URu<sub>2</sub>Si<sub>2</sub> exhibits a second order phase transition at  $T_{\text{HO}} \approx 17.5$  K. In spite of long-standing enormous efforts in experimental and theoretical studies[1–14], the order parameter of this phase transition has not yet been identified. The enigmatic features of this so-called "hidden order(HO)" phase are described as follows: (i) Despite large anomaly in thermodynamic quantities and drastic reconstruction of the Fermi surfaces at  $T = T_{\text{HO}}$ , there is neither conventional magnetic order nor the change of the crystal structure[1–3, 15–19]. (ii) However, under applied pressure, an antiferromagnetic (AF) state with large moment appears, and more surprisingly, the Fermi surfaces in the AF ordered state are almost the same as those found in the HO phase[20–24].

Recently, an experimental breakthrough for this issue was achieved by Okazaki et al.[25], who found spontaneous symmetry breaking in the spin space at  $T < T_{\text{HO}}$ . They reported that the anisotropy of the spin susceptibility in the  $xy$ -plane, which is measured by the quantity  $\chi_{xy} = \langle S_x S_y \rangle$ , becomes nonzero below  $T_{\text{HO}}$ . Since URu<sub>2</sub>Si<sub>2</sub> is tetragonal with four-fold symmetry at  $T > T_{\text{HO}}$ , and the phase transition at  $T = T_{\text{HO}}$  does not accompany any lattice distortion, it is reasonable to expect that this symmetry breaking is an essential feature of the HO phase, which imposes a crucial constraint on possible candidates of the HO parameter. Motivated by this experimental observation, in this letter, we discuss a possibility that a spin nematic (SN) state is realized as the hidden order in URu<sub>2</sub>Si<sub>2</sub>. The SN phase is a state with circulating spin currents, but with no magnetic moment[26–28]. The circulating spin currents break spin rotational symmetry, leading to spin anisotropy, without breaking time-reversal symmetry. We demonstrate that the above-mentioned features of the HO phase are naturally understood within the scenario of the SN order, and furthermore, that the temperature dependence of the spin anisotropy spontaneously generated in the SN state successfully explains the above experimental observation in a semi-quantitative way, providing strong evidence for the realization of the SN state as the HO phase

of URu<sub>2</sub>Si<sub>2</sub>.

We, first, present a mean field analysis for basic properties of the SN state applied to the case of URu<sub>2</sub>Si<sub>2</sub>. The SN state is induced by nesting of the Fermi surface as discussed in refs.[26, 27]. In fact, the recent band calculations for URu<sub>2</sub>Si<sub>2</sub> based on an itinerant  $f$ -electron picture revealed that there are one electron band denoted as  $\varepsilon_{\mathbf{k}_1}$  and one hole band denoted as  $\varepsilon_{\mathbf{k}_2}$ [22, 29], which are nested to each other via the nesting vector  $\mathbf{Q}_0 = (0, 0, \pi)$ : i.e.  $\varepsilon_{\mathbf{k}+\mathbf{Q}_0} = -\varepsilon_{\mathbf{k}}$ [30, 31]. It is noted that  $\mathbf{Q}_0$  is equivalent to the ordering vector of the large-moment AF state which is observed under applied pressure[20]. Moreover, it was pointed out that several experimental results suggest that the energy gap opens on the Fermi surface below  $T_{\text{HO}}$ [18, 32–35], which is consistent with the gap generation due to the nesting of the Fermi surface. Because of these reasons, we employ the scenario that itinerant  $f$ -electrons undergo the transition to the SN state triggered by the Fermi surface nesting. We will discuss the microscopic origin of this instability later. Since the ordering vectors for the large-moment AF phase and the SN phase are the same, the feature (ii) mentioned above is naturally understood within our scenario. The SN phase is a spin-triplet electron-hole pairing state[26, 27], and hence the order parameter of the SN state for the effective two band model is

$$\mathcal{O}_{\sigma\sigma'}^{\text{SN}}(\mathbf{k}) = \langle c_{\mathbf{k}_1\sigma}^\dagger c_{\mathbf{k}+\mathbf{Q}_0} c_{\mathbf{k}_2\sigma'} \rangle = \mathbf{d}_{12}(\mathbf{k}) \cdot \boldsymbol{\sigma}_{\sigma\sigma'}, \quad (1)$$

where  $c_{\mathbf{k}a\sigma}^\dagger$  ( $c_{\mathbf{k}a\sigma}$ ) is a creation (an annihilation) operator for an electron in the band  $a = 1, 2$  with momentum  $\mathbf{k}$ , spin  $\sigma$ .  $\mathbf{d}_{12}(\mathbf{k})$  is a vector, the direction of which is parallel to the spin quantization axis of the SN order. Because of time-reversal invariance in the SN state, we have the condition  $\mathbf{d}_{12}^*(-\mathbf{k}) = -\mathbf{d}_{12}(\mathbf{k})$ . Furthermore, we impose inversion symmetry, since there is no indication of broken inversion symmetry in URu<sub>2</sub>Si<sub>2</sub> from experiments. Then, it follows that  $\mathbf{d}_{12}^*(\mathbf{k}) = -\mathbf{d}_{12}(\mathbf{k})$ . Also, we assume that  $\mathbf{d}_{ab}(\mathbf{k})$  is symmetric with respect to the exchange of the band indices  $a$  and  $b$ . This assumption will be plausibly justified by a microscopic argument given later. The mean field Hamiltonian for the SN state of the effective

two-band model is  $\mathcal{H}_{\text{MF}} = \mathcal{H}_{\text{MF}}^{(0)} + \mathcal{H}_{\text{MF}}^{(1)}$  with the kinetic energy term  $\mathcal{H}_{\text{MF}}^{(0)} = \sum_{\mathbf{k}, \sigma} \sum_{a=1,2} \varepsilon_{\mathbf{k}a} c_{\mathbf{k}a\sigma}^\dagger c_{\mathbf{k}a\sigma}$ , and the particle-hole pairing term,

$$\mathcal{H}_{\text{MF}}^{(1)} = \sum_{\mathbf{k}, \sigma, \sigma'} \sum_{\substack{a,b \\ a \neq b}} [d_{ab}(\mathbf{k}) \cdot \sigma_{\sigma\sigma'} c_{\mathbf{k}+\mathbf{Q}_0 a\sigma}^\dagger c_{\mathbf{k}b\sigma'} + h.c.]. \quad (2)$$

For URu<sub>2</sub>Si<sub>2</sub>, the crystal structure of which has the  $D_{4h}$  symmetry, the anisotropy of the spin susceptibility which breaks four-fold symmetry down to two-fold symmetry in the  $xy$ -plane implies that the order parameter belongs to two-dimensional (2D) representation of the  $D_{4h}$  symmetry, and in the hidden order phase, four-fold symmetry in the 2D space is spontaneously broken. Then, from the symmetry properties of  $\mathbf{d}_{12}(\mathbf{k})$  discussed above, a possible candidate is the  $E_g$  state with  $\mathbf{d}_{12}(\mathbf{k}) = i(\Delta_1 k_y k_z, \Delta_2 k_x k_z, 0)$  (or  $i(\Delta_1 k_x k_z, \Delta_2 k_y k_z, 0)$ ) for small  $|\mathbf{k}|$ . Here, the real parameters  $\Delta_1$  and  $\Delta_2$  are determined from the self-consistent gap equation.

According to the experiment[25], the axis of the Ising-like anisotropy, which is spontaneously generated in the HO phase, is parallel to the (1,1,0)-direction. Since our toy model has continuous rotational symmetry in the  $xy$ -plane, the analysis given here is applicable to URu<sub>2</sub>Si<sub>2</sub> by rotating the principle axes by  $\pi/4$  around the  $z$ -axis, i.e.  $x' = \frac{1}{\sqrt{2}}(x - y)$  and  $y' = \frac{1}{\sqrt{2}}(x + y)$ . Following the experimental observation, we assume that four-fold symmetry in the  $x'y'$ -plane is spontaneously broken, resulting in the state with  $\mathbf{d}_{12}(\mathbf{k}) \parallel (1, 0, 0)$  or  $(0, 1, 0)$  in this rotated spin frame. The direction of  $\mathbf{d}_{12}(\mathbf{k})$  is determined by the detail of the electronic structure and spin-orbit interaction. However, most of the following results do not depend on it. For the tight-binding model, we choose

$$\mathbf{d}_{12}(\mathbf{k}) = (i\Delta_1 \phi(\mathbf{k}), 0, 0), \quad \phi(\mathbf{k}) = \sin k_{\mu'} \sin k_z, \quad (3)$$

where  $\mu' = x'$  or  $y'$ .

At this stage, we note that the electron-hole pairing term (2) is nonzero only when the nesting vector  $\mathbf{Q}_0$  and the momentum dependence of  $\mathbf{d}_{ab}(\mathbf{k})$  fulfill the following relation;  $e^{-i\mathbf{Q}_0 \mathbf{r}_i} - e^{i\mathbf{Q}_0 \mathbf{r}_j} \neq 0$  for  $\mathbf{r}_i, \mathbf{r}_j$  satisfying  $\Delta_{ij} = \sum_{\mathbf{k}} \phi(\mathbf{k}) e^{-i\mathbf{k}(\mathbf{r}_i - \mathbf{r}_j)} \neq 0$ . For (3) and  $\mathbf{Q}_0 = (0, 0, \pi)$ , this is actually fulfilled. It is instructive to compare this property of the SN phase with the unconventional spin density wave (USDW) state considered in refs. [3, 6], the order parameter of which is also given by Eq.(1) but with  $\mathbf{d}_{12}$  a real even function of  $\mathbf{k}$ , because of broken time-reversal symmetry. It is easy to see that, if  $\mathbf{Q}_0 = (0, 0, \pi)$ , and the momentum dependence of  $\mathbf{d}_{12}(\mathbf{k})$  is the same as (3), the particle-hole pairing term (2) vanishes, and hence, this type of the USDW can not be realized. It is noted that the USDW is more stabilized than the SN phase, if the order parameter  $\mathbf{d}_{ab}(\mathbf{k})$  (and hence, the particle-hole pairing interaction) is anti-symmetric with respect to the exchange of the band indices  $a, b$ , or if higher harmonics of the order parameter such as  $\phi(\mathbf{k}) = \sin 2k_{\mu'} \sin 2k_z$  is allowed.

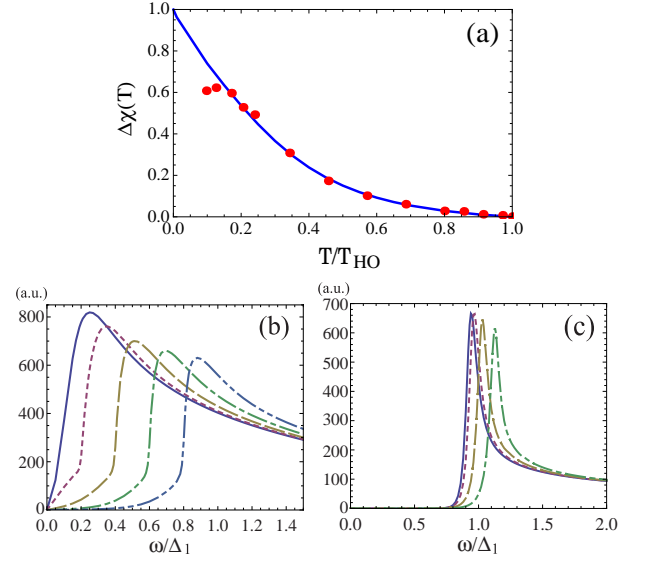


FIG. 1: (a) Solid line: anisotropy of the spin susceptibility  $\Delta\chi = \chi_{x'x'} - \chi_{y'y'}$  in the SN phase versus  $T/T_{\text{HO}}$ . The magnitude of  $\Delta\chi$  is normalized by the value at  $T = 0$ . Circle: experimental data quoted from [25].  $\Delta_1(0)/T_{\text{HO}} = 2.6$ . (b)  $\text{Im}\chi^{zz}(\mathbf{Q}_0, \omega)$  versus  $\omega/\Delta_1$ .  $\mu_B H_z/\Delta_1 = 0$  (solid), 0.1 (dotted), 0.2 (dashed), 0.3 (dot-dashed), 0.4 (double-dot-dashed). (c)  $\text{Im}\chi^{zz}(\mathbf{Q}_1, \omega)$  versus  $\omega/\Delta_1$ .  $\mu_B H_z/\Delta_1 = 0$  (solid), 0.1 (dotted), 0.2 (dashed), 0.3 (dot-dashed).

We, now, calculate the anisotropy of the uni-form spin susceptibility, which characterizes the SN order, and was experimentally detected in ref.[25]. The anisotropy in the  $x'y'$ -plane for our model is obtained as,  $\Delta\chi(T) \equiv \chi_{y'y'}(T) - \chi_{x'x'}(T) = \mu_B^2 \sum_{\mathbf{k}'} \left[ \frac{\tanh \frac{E_{\mathbf{k}'}}{2T}}{E_{\mathbf{k}'}} - \frac{1}{2T \cosh^2 \frac{E_{\mathbf{k}'}}{2T}} \right] \frac{|\mathbf{d}_{12}(\mathbf{k}')|^2}{4E_{\mathbf{k}'}}^2$  where  $E_{\mathbf{k}} = \sqrt{\varepsilon_{\mathbf{k}1}^2 + |\mathbf{d}_{12}(\mathbf{k})|^2}$ , and the momentum sum  $\sum_{\mathbf{k}'}$  is taken over the nested part of the Fermi surface satisfying the condition  $\varepsilon_{\mathbf{k}+\mathbf{Q}_0 1} = -\varepsilon_{\mathbf{k} 2}$ . Also, we assume the BCS mean-field-like  $T$ -dependence of the amplitude of the gap  $\Delta_1(T)$ . To make a semi-quantitative comparison with the experimental data without referring to the details of the band structure, we consider a ratio  $\Delta\chi(T)/\Delta\chi(0)$ , for which it is expected that effects of specific band structures approximately cancel out. There are two parameters in this calculation; one is the ratio of the energy gap at  $T = 0$  to the transition temperature, i.e.  $\Delta_1(0)/T_{\text{HO}}$ , and the other is an overall normalization factor of the magnitude. According to the recent scanning tunneling microscopy (STM) measurement, the magnitude of the gap opened on the Fermi surface via the hidden order transition is  $\Delta_1(0) \sim 4$  meV[32, 33]. Since  $T_{\text{HO}} = 17.5$  K, we choose the parameter as  $\Delta_1(0)/T_{\text{HO}} = 2.6$ . Then, there is only one fitting parameter, i.e. the overall normalization factor. We choose the normalization factor to fit the theoretical result at  $T = 6$  K to the experi-

mental data at the same temperature. The calculated result of this one-parameter fitting is shown in FIG.1(a). In spite of simplicity of the model, the theoretical result is surprisingly in good agreement with the experimental observations, at least above  $T/T_{\text{HO}} \sim 0.15$ . A slight discrepancy at low temperatures may be ascribed to the superconducting transition. This result provides strong evidence for the realization of the SN state as the HO in URu<sub>2</sub>Si<sub>2</sub>. In FIG.1(a), the  $T$ -linear behavior of  $\Delta\chi(T)$  at low temperatures is seen, which is raised by the existence of the line node of the order parameter (3). The experimental data is also consistent with this behavior above  $T/T_{\text{HO}} \sim 0.15$ .

The above scenario also has important implications for magnetic properties of the HO phase. According to neutron scattering measurements, there is a longitudinal spin fluctuation with the wave number  $\mathbf{q} = \mathbf{Q}_0$ , which exhibits an excitation gap in the HO phase [34]. Remarkably, the magnitude of the spin gap  $\sim 1.6$  meV is much smaller than the single particle energy gap  $\Delta_1 \sim 4$  meV observed via the STM measurements [32, 33]. Furthermore, the spin gap increases notably with increasing a magnetic field applied along the  $z$ -axis,  $H_z$ ; e.g. the spin gap for  $H_z = 17$  T reaches to 2.5 meV [34]. These properties are well explained by the present model. Using the mean field Hamiltonian  $\mathcal{H}_{\text{MF}}$  and the random phase approximation, we calculate the longitudinal spin correlation function  $\chi^{zz}(\mathbf{q}, \omega) = -i \int_0^\infty dt \langle [S^z(\mathbf{q}, t), S^z(-\mathbf{q}, 0)] \rangle e^{i\omega t}$  for  $\mathbf{q} = \mathbf{Q}_0$ , which is dominated by the transition between the band  $\varepsilon_{\mathbf{k}1}$  and the band  $\varepsilon_{\mathbf{k}2}$  [36]. In FIG. 1(b), the imaginary part of  $\chi^{zz}(\mathbf{Q}_0, \omega)$  is plotted as a function of the frequency  $\omega/\Delta_1$ , which indicates the spin excitation gap smaller than the single-electron gap  $\Delta_1$ . As the magnetic field  $H_z$  increases, the excitation gap increases substantially. These behaviors are understood as a result of the existence of line nodes of the gap  $|\mathbf{d}_{12}(\mathbf{k})|$ . The line nodes allow low-energy spin excitations to develop below  $\Delta_1$ . When the system is in the vicinity of magnetic criticality, a gap structure appears for  $\omega < \Delta_1$ , which is also sensitive to applied magnetic fields, as shown in FIG. 1(b). These results are in good agreement with the experimental observation obtained in ref.[34]. Conversely, these neutron scattering data strongly imply the existence of line-nodes in the energy gap. On the other hand, these experiments also revealed that in addition to  $\mathbf{Q}_0$ , there is a longitudinal incommensurate spin fluctuations with  $\mathbf{Q}_1 = (1.4\pi, 0, 0)$  [15], which may be attributed to the nesting between the hole band  $\varepsilon_{\mathbf{k}2}$  and another hole band denoted as  $\varepsilon_{\mathbf{k}3}$ , as suggested from the band calculations [22, 30]. According to the recent experiments, the magnetic excitation for the incommensurate  $\mathbf{Q}_1$  has an energy gap  $\sim 4$  meV below  $T_{\text{HO}}$ [18, 34, 37]. In our scenario, the gap  $\sim 4$  meV opens in the hole band  $\varepsilon_{\mathbf{k}2}$  in the SN state, while it does not in the hole band  $\varepsilon_{\mathbf{k}3}$ . Thus, the magnetic excitations due to the transition between these two hole bands should exhibit the excitation energy

gap  $\sim 4$  meV at the wave vector  $\mathbf{Q}_1$  rather than  $2 \times 4$  meV. This explains the above-mentioned experimental result. To demonstrate this, we calculate the spin correlation function  $\chi^{zz}(\mathbf{Q}_1, \omega)$  for the mean field Hamiltonian [36]. In this calculation, we postulate that hot spots on the hole band 2 for this spin fluctuation are located away from the gap-node of  $|\mathbf{d}_{12}(\mathbf{k})|$ ; i.e.  $|\mathbf{d}_{12}(\mathbf{k})| \neq 0$  for  $\mathbf{k}$  satisfying  $\varepsilon_{\mathbf{k}+\mathbf{Q}_1} \approx -\varepsilon_{\mathbf{k}3}$ . Then, the sharp gap edge appears at  $\omega = \Delta_1$  in  $\text{Im}\chi^{zz}(\mathbf{Q}_1, \omega)$ , as shown in FIG. 1(c). In the case with magnetic fields  $H_z$ , the gap edge shifts to  $\omega \approx \Delta_1 + 2H_z^2/\Delta_1$  [36]. Thus, the field dependence of  $\text{Im}\chi^{zz}(\mathbf{Q}_1, \omega)$  is much weaker than that of  $\text{Im}\chi^{zz}(\mathbf{Q}_0, \omega)$  (FIG. 1(c)). This is also qualitatively in agreement with the experimental results[34, 37].

Some remarks are in order: (i) In the SN state, there are staggered circulating spin currents [26, 27]. When a uniform magnetic field parallel to  $(1, 1, 0)$  or  $(1, -1, 0)$  in the original frame is applied, and electron spins are polarized, the spin currents lead to the staggered orbital currents, which induce staggered moment, as in the case of the orbital current state [7]. In NMR experiments, broadening of spectra under applied fields was observed [16, 17]. Its origin may be attributed to the staggered circulating currents of the SN state. The magnitude of the induced staggered field raised by the circulating currents is estimated as  $\sim 1$  Oe for the applied field  $H \sim 4$  T, which is consistent with the experimental results[17].

(ii) Note that the USDW state with the spin quantization axis parallel to  $(1, \pm 1, 0)$  also exhibits the same spin anisotropy as the SN state, and may explain the experimental data of ref.[25]. At this stage, we can not thoroughly exclude the possibility of the USDW as a candidate of the HO, though, as mentioned before, the particle-hole pairing interaction anti-symmetric with respect to the band indices, the origin of which is microscopically unclear, is required for its realization.

(iii) The SN order parameter couples to a magnetic field  $\mathbf{H}$  as  $\sim (\mathbf{d}_{12} \cdot \mathbf{H})^2$  in the free energy. This implies that the nonlinear susceptibility  $\chi_3$  for a magnetic field  $\mathbf{H}$  satisfying  $\mathbf{d}_{12} \cdot \mathbf{H} \neq 0$  exhibits a discontinuous jump at  $T = T_{\text{HO}}$  for the SN order (3). However, such an anomaly was experimentally observed not for the in-plane field, but for  $\mathbf{H} \parallel z$ -axis [3]. The discontinuous jump for  $\mathbf{H} \parallel z$ -axis may be explained by postulating that the SN vector  $\mathbf{d}_{12}$  is not confined in the  $xy$  plane, but rather has a nonzero out-of-plane component. This scenario may also explain the change of the slope of the linear spin susceptibility at  $T = T_{\text{HO}}$  for  $\mathbf{H} \parallel z$ -axis. However, the absence of the jump for the in-plane field in the experiment remains to be resolved. It is desirable to re-examine the measurement of the nonlinear susceptibility using recent high-quality samples.

(iv) According to specific heat measurements in magnetic fields parallel to the  $z$ -axis  $H_z$ , the specific heat jump  $\Delta C$  at  $T = T_{\text{HO}}$  is almost constant as a function of  $H_z$ , though the transition temperature decreases as

$T_{\text{HO}}(H_z) - T_{\text{HO}}(0) \propto -H_z^2$  [38, 39]. These behaviors are explained by the SN scenario. The decrease of  $T_{\text{HO}}$  is understood as a result of the decrease of the particle-hole pairing interaction due to the magnetic field [36]. Also, the absence of the change of  $\Delta C$  under applied fields is explained by taking into account the selfenergy correction arising from interactions with AF spin fluctuations [36]. Within this scenario, the specific heat jump is given by  $\Delta C \sim \xi^2 T_{\text{HO}}$ , where  $\xi$  is the correlation length for AF spin fluctuations. If the system is in the vicinity of the AF critical point, i.e.  $\xi^2 \sim 1/T$ ,  $\Delta C$  is constant, though  $T_{\text{HO}}$  is decreased by the magnetic field.

(v) Experimental studies reported that under applied pressure, the discontinuous phase transition from the HO state to the large moment AF state occurs [20], while the Fermi surfaces in both phases are almost the same [19, 21, 23, 24]. According to our scenario, there are competing AF spin fluctuations and fluctuations toward the SN phase transition in the system. (see below and Supplemental Material for details) Thus, applied pressure induces the change of effective couplings between electrons and these fluctuations, resulting in the transition to the AF phase. Since the order parameters of these phases have the different symmetries that are not compatible with continuous phase transition, the type of the phase transition is first-order, which is in agreement with experiments [17, 20]. We stress that the reconstructed Fermi surfaces in the SN phase and the AF phase are the same in our scenario, because both of them are reconstructed by the same nesting vector  $\mathbf{Q}_0$ . This is also in agreement with experimental observations [19, 21–24].

Finally, we discuss microscopic mechanism of the SN order for  $\text{URu}_2\text{Si}_2$  [36]. We consider a scenario that orbital fluctuations associated with the Fermi surface nesting yields the SN order. The minimal model consists of the three bands  $\varepsilon_{\mathbf{k}a}$  with  $a = 1, 2, 3$ , and mutual Coulomb interaction between electrons. The SN order considered here arises from the particle-hole pairings in the  $d$ -wave channel which are formed between the electron band 1 and the hole band 2. The Fermi surface nesting with the nesting vector  $\mathbf{Q}_0$  between these bands leads to this instability. An effective pairing interaction in the  $d_{\mu'z}$ -wave channel is mediated via orbital fluctuations arising from the Fermi surface nesting between  $\varepsilon_{\mathbf{k}3(1)}$  and  $\varepsilon_{\mathbf{k}2}$  with the nesting vector  $\mathbf{Q}_1$  ( $\mathbf{Q}_0$ ). If the orbital fluctuations are sufficiently strong, the SN order is stabilized [36].

In conclusion, we have demonstrated that the SN state induced by the Fermi surface nesting is a promising candidate of the HO phase of  $\text{URu}_2\text{Si}_2$ , since it successfully explains most of experimental observations including the recent experiment on four-fold symmetry-breaking.

The author thanks Y. Matsuda and T. Shibauchi for invaluable discussions, and kindly providing the author their experimental data. He is also indebted to A. V. Balatsky, P. M. Oppeneer, and A. Yazdani for useful dis-

cussions. This work is supported by the Grant-in-Aids for Scientific Research from MEXT of Japan (Grants No.19052003 and No.21102510).

- 
- [1] T. T. M. Palstra, A. A. Menovsky, J. van den Berg, A. J. Dirkmaat, P. H. Kes, G. J. Nieuwenhuys, and J. A. Mydosh, *Phys. Rev. Lett.* **55**, 2727 (1985).
  - [2] M. B. Maple, J. W. Chen, Y. Dalichaouch, T. Kohara, C. Rossel, M. S. Torikachvili, M. W. McElfresh, and J. D. Thompson, *Phys. Rev. Lett.* **56**, 185 (1986).
  - [3] A. P. Ramirez, P. Coleman, P. Chandra, E. Brück, A. A. Menovsky, Z. Fisk, and E. Bucher, *Phys. Rev. Lett.* **68**, 2680 (1992).
  - [4] V. Barzykin and L. P. Gor'kov, *Phys. Rev. Lett.* **70**, 2479 (1993).
  - [5] P. Santini and G. Amoretti, *Phys. Rev. Lett.* **73**, 1027 (1994).
  - [6] H. Ikeda and Y. Ohashi, *Phys. Rev. Lett.* **81**, 3723 (1998).
  - [7] P. Chandra, P. Coleman, J. A. Mydosh, and V. Tripathi, *Nature* **417**, 831 (2002).
  - [8] V. P. Mineev and M. E. Zhitomirsky, *Phys. Rev. B* **72**, 014432 (2005).
  - [9] A. Kiss and P. Fazekas, *Phys. Rev. B* **71**, 054415 (2005).
  - [10] C. M. Varma and L. Zhu, *Phys. Rev. Lett.* **96**, 036405 (2006).
  - [11] F. Cricchio, F. Bultmark, O. Grånäs, and L. Nordström, *Phys. Rev. Lett.* **103**, 107202 (2009).
  - [12] K. Haule and G. Kotliar, *Nature Phys.* **5**, 796 (2009).
  - [13] H. Harima, K. Miyake, and J. Flouquet, *J. Phys. Soc. Jpn.* **79**, 033705 (2010).
  - [14] Y. Dubi and A. V. Balatsky, *Phys. Rev. Lett.* **106**, 086401 (2011).
  - [15] C. Broholm, H. Lin, P. T. Matthews, T. E. Mason, W. J. L. Buyers, M. F. Collins, A. A. Menovsky, J. A. Mydosh, and J. K. Kjems, *Phys. Rev. B* **43**, 12809 (1991).
  - [16] K. Matsuda, Y. Kohori, T. Kohara, K. Kuwahara, and H. Amitsuka, *Phys. Rev. Lett.* **87**, 087203 (2001).
  - [17] S. Takagi, S. Ishihara, S. Saitoh, H. Sasaki, H. Tanida, M. Yokoyama, and H. Amitsuka, *J. Phys. Soc. Jpn.* **76**, 033708 (2007).
  - [18] C. R. Wiebe, J. A. Janik, G. J. MacDougall, G. M. Luke, J. D. Garrett, H. D. Zhou, Y. J. Jo, L. Balicas, Y. Qiu, J. R. D. Copley, et al., *Nature Phys.* **3**, 96 (2007).
  - [19] Y. J. Jo, L. Balicas, C. Capan, K. Behnia, P. Lejay, J. Flouquet, J. A. Mydosh, and P. Schlottmann, *Phys. Rev. Lett.* **98**, 166404 (2007).
  - [20] H. Amitsuka, K. Matsuda, I. Kawasaki, K. Tenya, M. Yokoyama, C. Sekine, N. Tateiwa, T. C. Kobayashi, S. Kawarazaki, and H. Yoshizawa, *J. Mag. Mag. Mater.* **330**, 214 (2007).
  - [21] M. Nakashima, H. Ohkuni, Y. Inada, R. Settai, Y. Haga, E. Yamamoto, and Y. Onuki, *J. Phys.: Condens. Matter* **15**, S2011 (2003).
  - [22] S. Elgazzar, J. Rusz, M. Amft, P. M. Oppeneer, and J. A. Mydosh, *Nature Mater.* **8**, 337 (2009).
  - [23] E. Hassinger, G. Knebel, T. D. Matsuda, D. Aoki, V. Taufour, and J. Flouquet, *Phys. Rev. Lett.* **105**, 216409 (2010).
  - [24] R. Yoshida, Y. Nakamura, M. Fukui, Y. Haga, E. Ya-

- mamoto, Y. Ōnuki, M. Okawa, S. Shin, M. Hirai, Y. Muraoka, et al., Phys. Rev. B **82**, 205108 (2010).
- [25] R. Okazaki, T. Shibauchi, H. J. Shi, Y. Haga, T. D. Matsuda, E. Yamamoto, Y. Onuki, H. Ikeda, and Y. Matsuda, Science **331**, 439 (2011).
- [26] H. J. Schulz, Phys. Rev. B **39**, 2940 (1989).
- [27] A. A. Nersisyan, G. I. Japaridze, and I. G. Kimeridze, J. Phys.: Condens. Matter **3**, 3353 (1991).
- [28] The SN state considered here is different from the nematic state of Sr<sub>3</sub>Ru<sub>2</sub>O<sub>7</sub> [see, e.g., E. Fradkin, S. A. Kivelson, M. J. Lawler, J. P. Eisenstein, and A. P. Mackenzie, Annu. Rev. Condensed Matter Phys. **1**, 153 (2010)] in that the former breaks rotational symmetry mainly in the spin space, while the latter breaks it in the momentum space, and that the former is raised by gap opening on the Fermi surface, while the latter is realized by the Pomeranchuk instability without gap formation.
- [29] M. Biasini, J. Ruzs, and A. P. Mills, Phys. Rev. B **79**, 085115 (2009).
- [30] P. M. Oppeneer, J. Ruzs, S. Elgazzar, M.-T. Suzuki, T. Durakiewicz, and J. A. Mydosh, Phys. Rev. B **82**, 205103 (2010).
- [31] P. M. Oppeneer, private communication.
- [32] P. Aynajian, E. da Silva Neto, C. V. Parker, Y. Huang, A. Pasupathy, J. Mydosh, and A. Yazdani, PNAS **107**, 10383 (2010).
- [33] A. R. Schmidt, M. H. Hamidian, P. Wahl, F. Meier, A. V. Balatsky, J. D. Garrette, T. J. Williams, and G. M. Luke, Nature **465**, 570 (2010).
- [34] F. Bourdarot, B. Fåk, K. Habicht, and K. Prokeš, Phys. Rev. Lett. **90**, 067203 (2003).
- [35] A. F. Santander-Syro, M. Klein, F. L. Boariu, A. Nuber, P. Lejay, and F. Reinert, Nature Phys. **5**, 637 (2009).
- [36] For the details, see Supplemental Material.
- [37] F. Bourdarot, E. Hassinger, S. Raymond, D. Aoki, V. Taufour, L. P. Regnault, and J. Flouquet, J. Phys. Soc. Jpn. **79**, 064719 (2010).
- [38] N. H. van Dijk, F. Bourdarot, J. C. P. Klaasse, I. H. Hagmusa, E. Brück, and A. A. Menovsky, Phys. Rev. B **56**, 14493 (1997).
- [39] M. Jaime, K. H. Kim, G. Jorge, S. McCall, and J. A. Mydosh, Phys. Rev. Lett. **89**, 287201 (2002).
- [40] Y. Tada, N. Kawakami, and S. Fujimoto, Phys. Rev. B **81**, 104506 (2010).

## SUPPLEMENTAL MATERIAL

### A. Spin correlation functions in the spin nematic state

In this section, we present the calculations of the dynamical longitudinal spin correlation functions  $\chi^{zz}(\mathbf{q}, \omega)$  in the SN state, particularly focusing on the modes with  $\mathbf{q} = \mathbf{Q}_0$  or  $\mathbf{Q}_1$ , for which spin fluctuations are prominent. The minimal model consists of the three bands,  $\varepsilon_{\mathbf{k}1}$ ,  $\varepsilon_{\mathbf{k}2}$ , and  $\varepsilon_{\mathbf{k}3}$ , with the particle-hole pairing term, and the mutual Coulomb interaction between electrons

in these bands. The Hamiltonian is

$$\begin{aligned} \mathcal{H} = & \sum_{\mathbf{k}, \sigma, a} \varepsilon_{\mathbf{k}a} c_{\mathbf{k}a\sigma}^\dagger c_{\mathbf{k}a\sigma} \\ & + \sum_{\mathbf{k}, \sigma, \sigma'} \sum_{\substack{a, b \\ a \neq b}} [\mathbf{d}_{ab}(\mathbf{k}) \cdot \boldsymbol{\sigma}_{\sigma\sigma'} c_{\mathbf{k}+\mathbf{Q}_0 a \sigma}^\dagger c_{\mathbf{k} b \sigma'} + h.c.] \\ & + \sum_{\substack{\mathbf{k}, \mathbf{k}', \mathbf{q} \\ a, b, c, d, \sigma_i}} U_{\sigma_1 \sigma_2 \sigma_3 \sigma_4}^{abcd} c_{\mathbf{k}+\mathbf{q} a \sigma_1}^\dagger c_{\mathbf{k}'-\mathbf{q} b \sigma_2}^\dagger c_{\mathbf{k}' c \sigma_3} c_{\mathbf{k} d \sigma_4}, \end{aligned} \quad (4)$$

with  $a, b, c, d = 1, 2, 3$ . The SN order occurs for electrons in the band 1 and the band 2, i.e.  $|\mathbf{d}_{12}(\mathbf{k})| = |\mathbf{d}_{21}(\mathbf{k})| \neq 0$ , and  $|\mathbf{d}_{ab}(\mathbf{k})| = 0$  for other  $a, b$ .

Following the results of the recent band calculation[31], we postulate that the three bands,  $\varepsilon_{\mathbf{k}1}$ ,  $\varepsilon_{\mathbf{k}2}$ , and  $\varepsilon_{\mathbf{k}3}$ , have the orbital character with  $J_z = \pm 5/2$ ,  $\pm 3/2$ , and  $\pm 1/2$ , respectively, and that each of the single electron states in the  $a$ -th band with spin  $\sigma$  denoted as  $|a \sigma\rangle$  approximately corresponds to the orbital state  $|J_z\rangle$ . That is,

$$|1 \uparrow\rangle = |J_z = 5/2\rangle, \quad |1 \downarrow\rangle = |-5/2\rangle, \quad (5)$$

$$|2 \uparrow\rangle = |3/2\rangle, \quad |2 \downarrow\rangle = |-3/2\rangle, \quad (6)$$

$$|3 \uparrow\rangle = |1/2\rangle, \quad |3 \downarrow\rangle = |-1/2\rangle. \quad (7)$$

The interaction term of (4) conserve the total  $J_z$  in each scattering process. We, furthermore, assume that in the interaction term of (4), interactions between electrons with anti-parallel spins dominates over those between electrons with parallel spins, and neglect the latter. Then, nonzero coupling constants for the interaction between electrons in the band 1 and the band 2 are,

$$U_{\uparrow\downarrow\uparrow}^{aabb}, \quad U_{\downarrow\uparrow\downarrow}^{aabb}, \quad U_{\uparrow\downarrow\downarrow}^{abba}, \quad U_{\downarrow\uparrow\uparrow}^{abba}, \quad (8)$$

with  $(a, b) = (1, 2)$  or  $(2, 1)$ . For simplicity, we assume that all of these coupling constants are the same, and equal to  $U_{12}$ . Since we are concerned with effects of an applied magnetic field  $H$ , we also add the Zeeman term  $-g\mu_B S^z H$  to the Hamiltonian (4). Assuming the perfect nesting condition  $\varepsilon_{\mathbf{k}+\mathbf{Q}_0 1} = -\varepsilon_{\mathbf{k}2}$ , we write down the non-interacting single-electron Green function for the band 1 with spin  $\sigma$  in the SN state,  $G_{\mathbf{k}1\sigma}(\varepsilon_n)$ , in the following forms,

$$G_{\mathbf{k}1\sigma}(\varepsilon_n) = \frac{i\varepsilon_n + \varepsilon_{\mathbf{k}1} - s_\sigma h}{(i\varepsilon_n)^2 - E_{k\sigma}^2}, \quad (9)$$

where  $h = g\mu_B H$  and  $E_{k\sigma} = \sqrt{(\varepsilon_{\mathbf{k}1} - s_\sigma h)^2 + |\mathbf{d}_{12}(\mathbf{k})|^2}$  with  $s_\sigma = +1$  for  $\sigma = \uparrow$  and  $-1$  for  $\sigma = \downarrow$ . The Green functions for the band 2 are

$$G_{\mathbf{k}2\uparrow}(\varepsilon_n) = -G_{\mathbf{k}1\downarrow}(-\varepsilon_n), \quad (10)$$

$$G_{\mathbf{k}2\downarrow}(\varepsilon_n) = -G_{\mathbf{k}1\uparrow}(-\varepsilon_n). \quad (11)$$

The non-interacting anomalous Green functions generated by the SN order are given by,

$$F_{\mathbf{k}\uparrow\downarrow}(\varepsilon_n) = \int_0^\beta d\tau \langle T \{ c_{\mathbf{k}1\uparrow} c_{\mathbf{k}2\downarrow}^\dagger \} \rangle e^{i\omega_n \tau} = \frac{-i|\mathbf{d}_{12}(\mathbf{k})|}{(i\varepsilon_n)^2 - E_{k\uparrow}^2} \quad (12)$$

$$F_{\mathbf{k}\downarrow\uparrow}(\varepsilon_n) = \int_0^\beta d\tau \langle T \{ c_{\mathbf{k}\downarrow} c_{\mathbf{k}\uparrow}^\dagger \} \rangle e^{i\omega_n \tau} = \frac{i|\mathbf{d}_{12}(\mathbf{k})|}{(i\varepsilon_n)^2 - E_{\mathbf{k}\downarrow}^2} \quad (13)$$

The longitudinal spin correlation function enhanced by nesting between the band 1 and the band 2 is

$$\begin{aligned} \chi_{12}^{zz}(\mathbf{q}, \omega_n) &= \chi_{1221}^{zz}(\mathbf{q}, \omega_n) + \chi_{2112}^{zz}(\mathbf{q}, \omega_n) \\ &+ \chi_{1212}^{zz}(\mathbf{q}, \omega_n) + \chi_{2121}^{zz}(\mathbf{q}, \omega_n) \\ &= 2[\chi_{1221}^{zz}(\mathbf{q}, \omega_n) + \chi_{2121}^{zz}(\mathbf{q}, \omega_n)], \quad (14) \end{aligned}$$

where

$$\chi_{abcd}^{zz}(\mathbf{q}, \omega_n) = \int_0^\beta d\tau \langle T \{ S_{ab}^z(\mathbf{q}, \tau) S_{cd}^z(-\mathbf{q}, 0) \} \rangle e^{i\omega_n \tau} \quad (15)$$

with  $S_{ab}^z(\mathbf{q}) = \frac{1}{2} \sum_{\mathbf{k}} (c_{\mathbf{k}+\mathbf{q}a}^\dagger c_{\mathbf{k}b\uparrow} - c_{\mathbf{k}+\mathbf{q}a\downarrow}^\dagger c_{\mathbf{k}b\downarrow})$ . In the second equality of (14), we used the relations  $\chi_{1221}^{zz} = \chi_{2112}^{zz}$  and  $\chi_{1212}^{zz} = \chi_{2121}^{zz}$ .

Within the random phase approximation,  $\chi_{12}^{zz}$  is given by

$$\chi_{12}^{zz}(\mathbf{q}, \omega_n) = \frac{\chi_{12}^{(0)}(\mathbf{q}, \omega_n)}{1 - U_{12}\chi_{12}^{(0)}(\mathbf{q}, \omega_n)}, \quad (16)$$

where  $\chi_{12}^{(0)}(\mathbf{q}, \omega_n)$  is the spin correlation function in the case without Coulomb interaction. For  $\mathbf{q} = \mathbf{Q}_0$ , it is given by,

$$\begin{aligned} \chi_{12}^{(0)}(\mathbf{Q}_0, \omega_n) &= -\frac{T}{4} \sum_m \sum_{\mathbf{k}} \left[ \sum_{\sigma=\uparrow,\downarrow} G_{\mathbf{k}1\sigma}(\varepsilon_m) G_{\mathbf{k}2\sigma}(\varepsilon_m + \omega_n) \right. \\ &\left. - F_{\mathbf{k}\uparrow\downarrow}(\varepsilon_m) F_{\mathbf{k}\downarrow\uparrow}(\varepsilon_m + \omega_n) - F_{\mathbf{k}\downarrow\uparrow}(\varepsilon_m) F_{\mathbf{k}\uparrow\downarrow}(\varepsilon_m + \omega_n) \right] \\ &= \sum_{\mathbf{k}} \left[ \frac{\tanh \frac{E_{\mathbf{k}\uparrow}}{2T} + \tanh \frac{E_{\mathbf{k}\downarrow}}{2T}}{(E_{\mathbf{k}\uparrow} + E_{\mathbf{k}\downarrow})^2 - (i\omega_n)^2} (E_{\mathbf{k}\uparrow} + E_{\mathbf{k}\downarrow}) u_+(\mathbf{k}) \right. \\ &\left. + \frac{\tanh \frac{E_{\mathbf{k}\uparrow}}{2T} - \tanh \frac{E_{\mathbf{k}\downarrow}}{2T}}{(E_{\mathbf{k}\uparrow} - E_{\mathbf{k}\downarrow})^2 - (i\omega_n)^2} (E_{\mathbf{k}\uparrow} - E_{\mathbf{k}\downarrow}) u_-(\mathbf{k}) \right], \quad (17) \end{aligned}$$

where

$$u_{\pm}(\mathbf{k}) = \frac{1}{4} \left( 1 \pm \frac{\varepsilon_{\mathbf{k}1}^2 + |\mathbf{d}_{12}(\mathbf{k})|^2 - h^2}{E_{\mathbf{k}\uparrow} E_{\mathbf{k}\downarrow}} \right). \quad (18)$$

$\text{Im}\chi^{zz}(\mathbf{Q}_0, \omega)$  is approximately given by the retarded spin correlation function  $\text{Im}\chi_{12}^{zzR}(\mathbf{Q}_0, \omega)$ .

In a similar manner, we can obtain  $\chi^{zz}(\mathbf{Q}_1, \omega)$ , which is dominated by the longitudinal spin correlation function enhanced by nesting between the band 2 and the band 3,

$$\chi_{23}^{zz}(\mathbf{q}, \omega_n) = 2[\chi_{2332}^{zz}(\mathbf{q}, \omega_n) + \chi_{2323}^{zz}(\mathbf{q}, \omega_n)]. \quad (19)$$

From Eqs.(6) and (7) and the conservation of  $J_z$  in interaction processes, we see that nonzero coupling constants of the interaction between electrons in the band 2 and the band 3 are given by Eq.(8) with  $(a, b) = (2, 3)$  or  $(3, 2)$ . We assume that all of them are equal to  $U_{23}$ . To simplify the calculation, we also impose the perfect nesting condition  $\varepsilon_{\mathbf{k}+\mathbf{Q}_1, 2} = -\varepsilon_{\mathbf{k}3}$ . Since the energy gap does

not open in the band 3 in our model, we obtain within the random phase approximation,

$$\chi_{23}^{zz}(\mathbf{q}, \omega_n) = \frac{\chi_{23}^{(0)}(\mathbf{q}, \omega_n)}{1 - U_{23}\chi_{23}^{(0)}(\mathbf{q}, \omega_n)}, \quad (20)$$

where

$$\begin{aligned} \chi_{23}^{(0)}(\mathbf{q}, \omega_n) &= \sum_{\mathbf{k}, \sigma} \left[ \frac{\tanh \frac{E_{\mathbf{k}\sigma}}{2T} + \tanh \frac{\varepsilon_{\mathbf{k}1} + s_\sigma h}{2T}}{i\omega_n + E_{\mathbf{k}\sigma} + \varepsilon_{\mathbf{k}1} + s_\sigma h} w_+(\mathbf{k}) \right. \\ &\left. - \frac{\tanh \frac{E_{\mathbf{k}\sigma}}{2T} - \tanh \frac{\varepsilon_{\mathbf{k}1} + s_\sigma h}{2T}}{i\omega_n - E_{\mathbf{k}\sigma} + \varepsilon_{\mathbf{k}1} + s_\sigma h} w_-(\mathbf{k}) \right], \quad (21) \end{aligned}$$

with

$$w_{\pm}(\mathbf{k}) = \frac{1}{4} \left( 1 \pm \frac{\varepsilon_{\mathbf{k}1} - s_\sigma h}{E_{\mathbf{k}\sigma}} \right). \quad (22)$$

$\text{Im}\chi^{zz}(\mathbf{Q}_1, \omega)$  is approximated by  $\text{Im}\chi_{23}^{zzR}(\mathbf{Q}_1, \omega)$ .

Plots of  $\text{Im}\chi_{12}^{zzR}(\mathbf{Q}_0, \omega)$  and  $\text{Im}\chi_{23}^{zzR}(\mathbf{Q}_1, \omega)$  as functions  $\omega$  are shown in FIG.1(b) and (c), respectively, in the main text.

## B. Microscopic mechanism of the spin nematic state

In this section, we discuss microscopic mechanism of the SN order for URu<sub>2</sub>Si<sub>2</sub>. We consider a scenario that spin fluctuations and orbital fluctuations associated with the Fermi surface nesting with the nesting vectors  $\mathbf{Q}_0$  and  $\mathbf{Q}_1$  give rise to the phase transition to the SN order. Our argument is based on the three band model (4).

The spin fluctuations and the orbital fluctuations with the propagating wave numbers  $\mathbf{Q}_0$  and  $\mathbf{Q}_1$  mediate the effective interactions between electrons,

$$\mathcal{S}_{\text{int}} = \sum_{\substack{\mathbf{k}, \mathbf{k}', \mathbf{q} \\ a, b, c, d, \sigma_i}} \Gamma_{\sigma_1 \sigma_2 \sigma_3 \sigma_4}^{abcd}(\mathbf{q}) c_{\mathbf{k}+\mathbf{q}a\sigma_1}^\dagger c_{\mathbf{k}'-\mathbf{q}b\sigma_2}^\dagger c_{\mathbf{k}'c\sigma_3} c_{\mathbf{k}d\sigma_4} \quad (23)$$

with  $\mathbf{q} = (\mathbf{q}, \omega)$ .

From Eqs.(5), (6), and (7), and the conservation of the total  $J_z$  in each scattering process, the effective interaction that mediates the particle-hole pairing characterizing the SN order is approximately given by,

$$\begin{aligned} \Gamma_{\uparrow\downarrow\uparrow}^{2211}(q) &= \Gamma_{\uparrow\downarrow\uparrow}^{2211(0)}(q) - g_{\uparrow\uparrow\uparrow\uparrow}^{1212} g_{\downarrow\uparrow\uparrow\downarrow}^{2211} [\chi_{\uparrow\uparrow}^{12}(q) + \chi_{\downarrow\downarrow}^{12}(q)] \\ &- g_{\uparrow\uparrow\uparrow\uparrow}^{2231} g_{\downarrow\uparrow\uparrow\downarrow}^{2321} [\chi_{\uparrow\uparrow}^{23}(q) + \chi_{\downarrow\downarrow}^{23}(q)]. \quad (24) \end{aligned}$$

Here, the second and third terms are the interactions mediated via the orbital fluctuations which is characterized by the orbital susceptibility,

$$\chi_{\sigma\sigma}^{ab}(q) = \int_0^\beta d\tau \langle T \{ N_{ab\sigma}(\mathbf{q}, \tau) N_{ba\sigma}(-\mathbf{q}, 0) \} \rangle e^{i\omega_n \tau}, \quad (25)$$

where  $N_{ab\sigma}(\mathbf{q}) = \sum_{\mathbf{k}} c_{\mathbf{k}+\mathbf{q}a\sigma}^\dagger c_{\mathbf{k}b\sigma} \cdot g_{\uparrow\uparrow\uparrow\uparrow}^{1212}, g_{\downarrow\uparrow\uparrow\downarrow}^{2211}, g_{\uparrow\downarrow\downarrow\uparrow}^{2321}$  and  $g_{\downarrow\uparrow\uparrow\downarrow}^{2321}$  are effective coupling constants for interactions between the orbital fluctuations and electrons, which preserve  $J_z$ . The first term of (24) is the other interaction processes. The Fermi surface nesting between the band 1(3) and the band 2 with the nesting vector  $\mathbf{Q}_0$  ( $\mathbf{Q}_1$ ) enhances the orbital-fluctuation-mediated part of (24), while the first term of (24) is not much affected by it. In Eq.(24), we have neglected the interaction processes that are mediated by orbital fluctuations associated with  $\chi_{\uparrow\downarrow}^{ab}(q)$  and  $\chi_{\downarrow\uparrow}^{ab}$ , because these orbital fluctuations accompany transverse spin fluctuations, and, according to neutron scattering measurements, transverse spin fluctuations are fully suppressed in URu<sub>2</sub>Si<sub>2</sub>. [15] The second and third terms of (24) give rise to the particle-hole pairing interaction in the  $d_{\mu'z}$ -wave channel  $V_d \equiv \sum_{\mathbf{k}, \mathbf{k}'}^{\text{F.S.}} \phi(\mathbf{k})\phi(\mathbf{k}')\Gamma_{\uparrow\downarrow\uparrow\downarrow}^{2211}(\omega_n, \mathbf{k} - \mathbf{k}')$ . Here  $\sum_{\mathbf{k}, \mathbf{k}'}^{\text{F.S.}}$  denotes the momentum sum over the Fermi surfaces. Since  $\sum_{\mathbf{k}} \phi(\mathbf{k})\phi(\mathbf{k} + \mathbf{Q}_m) < 0$  with  $m = 0, 1$ , and the orbital susceptibility (25) is significantly enhanced at  $\mathbf{q} = \mathbf{Q}_1$  (or  $\mathbf{Q}_0$ ), the sign of  $V_d$  is positive, which leads to the  $d$ -wave particle-hole pairing characterizing the SN state.

In addition to (24), there is another important interaction channel which is related to the instability toward antiferromagnetism with staggered magnetization parallel to the  $z$ -axis. This instability is also driven by the Fermi surface nesting between the band 1 and the band 2, as in the case of the SN order [30]. We denote this effective interaction as  $\Gamma_{\uparrow\downarrow\uparrow\downarrow}^{2211}(q)$ . Note that  $\Gamma_{\uparrow\downarrow\uparrow\downarrow}^{2211}(q)$  is not enhanced by the orbital fluctuations associated with the orbital correlation function (25). Thus, if the orbital fluctuations are sufficiently strong, the effective interaction (24) gives rise to the instability toward the SN state. The transition temperature of the SN order within a mean field approximation is determined by the self-consistent gap equation,

$$\Delta_1 = V_d \sum_{\mathbf{k}} \phi^2(\mathbf{k}) \frac{\tanh(\frac{E_{\mathbf{k}}}{2T})}{E_{\mathbf{k}}} \Delta_1 / \sum_{\mathbf{k}} \phi^2(\mathbf{k}). \quad (26)$$

When there is an applied magnetic field parallel to the  $z$ -axis, the orbital susceptibility (25) is reduced. For a small field  $H_z$ , the nonzero lowest order correction is  $\delta\chi_{\sigma\sigma}^{ab}(q) \sim -c_0(q)H_z^2$  with  $c_0(q)$  a function of  $q$ . The magnetic field parallel to the  $z$ -axis affects the self-consistent gap equation (26) only through the effective pairing interaction. Thus, the transition temperature in the case with  $H_z$  behaves like  $T_{\text{HO}}(H_z) \sim T_{\text{HO}}(0) - a_0 H_z^2$  with  $a_0$  a positive constant. This field dependence of the transition temperature is actually observed in experiments [38].

### C. Specific heat jump

In this section, we discuss the specific heat jump at the HO transition point. According to specific heat measurements under magnetic fields applied along the  $z$ -axis, the specific heat jump  $\Delta C$  at  $T = T_{\text{HO}}$  is almost constant as a function of the magnetic fields, though the transition temperature decreases as  $T_{\text{HO}}(H_z) \sim T_{\text{HO}}(0) - a_0 H_z^2$ , as mentioned in the previous section [38, 39]. The constant specific heat jump is unusual for the itinerant  $f$ -electron system, since in the Fermi liquid state, the entropy generally decreases as  $T$  decreases. However, here, we show that this remarkable feature is explained by taking into account the selfenergy corrections arising from AF spin fluctuations. We start from the Ginzburg-Landau (GL) free energy in the vicinity of the HO transition point,  $\mathcal{F} = a\psi^2 + b\psi^4$ , with  $\psi$  the order parameter for the SN state. We have chosen the spin quantization axis parallel to  $\mathbf{d}_{12}$ . Thus,  $\psi = \Delta_1$  is a scalar order parameter. The specific heat jump at  $T = T_{\text{HO}}$  is given by

$$\Delta C = \frac{T_{\text{HO}}}{2b} \left( \frac{\partial a}{\partial T} \right)^2 \Big|_{T=T_{\text{HO}}}. \quad (27)$$

The coefficients of the GL free energy  $a$  and  $b$  are calculated from the normal Green functions,

$$G_{\mathbf{k}1\sigma}(\varepsilon_n) = \frac{1}{Z_{\mathbf{k}}(\varepsilon_n)i\varepsilon_n - \varepsilon_{\mathbf{k}1}} \quad (28)$$

with

$$Z_{\mathbf{k}}(\varepsilon_n) = 1 - \frac{1}{i\varepsilon_n} \Sigma_{\mathbf{k}}(\varepsilon_n), \quad (29)$$

and  $\Sigma_{\mathbf{k}}(\varepsilon_n)$  the selfenergy, and  $G_{\mathbf{k}2\sigma}(\varepsilon_n)$  which is obtained from the relations (10) and (11). The results are

$$a = \frac{1}{g} - \Pi(\mathbf{Q}_0), \quad (30)$$

with

$$\Pi(\mathbf{Q}_0) = -T \sum_{|n| \leq n_c} \sum_{\mathbf{k}} \phi^2(\mathbf{k}) G_{\mathbf{k}1\sigma}(\varepsilon_n) G_{\mathbf{k}+\mathbf{Q}_0 2-\sigma}(\varepsilon_n) \quad (31)$$

and

$$b = T \sum_{|n| \leq n_c} \sum_{\mathbf{k}} \phi^4(\mathbf{k}) [G_{\mathbf{k}1\sigma}(\varepsilon_n) G_{\mathbf{k}+\mathbf{Q}_0 2-\sigma}(\varepsilon_n)]^2. \quad (32)$$

Here  $n_c = E_c/T$  with  $E_c$  an energy cutoff for the effective particle-hole pairing interaction  $g$ . For simplicity, we neglect  $\mathbf{k}$ -dependence of  $Z_{\mathbf{k}}(\varepsilon_n)$ . Then, from eqs.(27), (31), and (32), we obtain,

$$\Delta C \approx N(0)Z(E_c)T_{\text{HO}}, \quad (33)$$

where  $N(0)$  is the density of states at the Fermi level. The selfenergy corrections  $Z(E_c)$  mainly stem from interactions with AF spin fluctuations and orbital fluctuations. Note that the AF spin fluctuations expressed by

(14) and (19) and the orbital fluctuations characterized by (25) are not independent, but deeply correlated. The former contributions generally enhance the latter, and vice versa. We postulate that the normal selfenergy corrections are mainly due to the interaction with the AF spin fluctuations with  $\mathbf{Q}_0$ , while the particle-hole pairing interaction (24) is dominated by the fluctuations with  $\mathbf{q} \sim \mathbf{Q}_1$ ; i.e. in Eq.(24), the coupling strength of the second term is much smaller than that of the third one, though the correlation length for the spin fluctuations with  $\mathbf{Q}_0$  is larger than that with  $\mathbf{Q}_1$ . We also assume that the characteristic energy scale of the AF spin fluctuations with  $\mathbf{q} = \mathbf{Q}_0$  is sufficiently larger than the Zeeman energy of the applied fields, and the AF spin fluctuations with  $\mathbf{Q}_0$  is not much affected by the magnetic fields, at least, in the vicinity of  $T \sim T_{\text{HO}}$ . The most important effect on  $Z(\varepsilon_n)$  in the vicinity of the transition temperature is the quasiparticle damping  $\gamma$ . If the system is suf-

ficiently clean, the quasiparticle damping raised by the interaction with the three-dimensional AF spin fluctuations with  $\mathbf{Q}_0$  is  $\gamma \sim \xi^2[\varepsilon_n^2 + (\pi T)^2]$  with  $\xi$  the correlation length for the AF spin fluctuations [40]. Then, from (33), we have  $\Delta C \sim \xi^2 T_{\text{HO}}$  up to a constant factor. If the system is in the vicinity of the AF quantum critical point, i.e.  $\xi^2 \sim 1/T$ ,  $\Delta C$  does not depend on  $T_{\text{HO}}$ . This result provides a possible explanation for the above-mentioned experimental observation that the specific heat jump at  $T = T_{\text{HO}}$  is not changed by the magnetic field, though the transition temperature is decreased by the magnetic field as  $T_{\text{HO}}(H_z) \sim T_{\text{HO}}(0) - a_0 H_z^2$  [38, 39]. We note that the above scenario of the constant specific heat jump is valid as long as  $T_{\text{HO}}(H_z)$  is sufficiently large compared to the change of the characteristic energy of the spin fluctuation raised by the magnetic field. Thus, when  $T_{\text{HO}}(H_z)$  is decreased too much by the applied field, the deviation from the above result may appear.